4-1-2018

Versatile Sarcosine Biosensing Schemes Utilizing Layer-by-Layer Construction of Carbon Nanotube-Chitosan Composite Films

Michael J. Pannell

Elizabeth E. Doll

Najwa Labban

Mulugeta B. Wayu

Julie A. Pollack

See next page for additional authors

Recommended Citation

M. Pannell, E. Doll, N. Labban, M. Wayu, J. Pollock, and M.C. Leopold, "Versatile Sarcosine and Creatinine Biosensing Schemes Utilizing Layer-by-Layer Construction of Carbon Nanotube-Chitosan Composite Films," *J. Electroanal. Chem.* 2018, *814*, 20-30. DOI: https://doi.org/10.1016/j.jelechem.2018.02.023

Versatile Sarcosine Biosensing Schemes Utilizing Layer-by-Layer Construction of Carbon Nanotube-Chitosan Composite Films

Michael J. Pannell, Elizabeth E. Doll, Najwa Labban, Mulugeta B. Wayu, Julie A. Pollock,* and Michael C. Leopold*

Abstract

Layer-by-layer composite films of carbon nanotubes (CNTs) within a chitosan matrix with sarcosine oxidase enzyme and capped with Nafion have been developed and optimized as a versatile 1st generation amperometric sarcosine biosensing platform that operates successfully both as an isolated sarcosine sensor as well as a functional component within a creatinine sensor. Accurate measurement of sarcosine in urine and creatinine in blood may help with early diagnosis of diseases such as prostate cancer and renal failure, respectively. In this study, each material within the film is systematically optimized toward sarcosine sensitivity, including a critical evaluation of different CNTs effect on sensing performance. Films featuring carboxylic acid–modified single–walled carbon nanotubes and strategic enzyme doping were shown to be most effective sarcosine sensing platforms, exhibiting excellent sensitivity (~0.5 μA/mM), a linear response (≤ 0.75 mM), fast response time (8 s), low limits of detection (~6 μM), as well as both continuous use stability (7 days) and effective shelf life (> 12 days). Operation of the sarcosine sensor was demonstrated in a urine matrix, detecting sarcosine at physiologically relevant concentrations and successfully quantifying sarcosine-spiked urine samples with high percent recovery and low relative error. The sarcosine sensing platform was also adapted to a 1st generation creatinine biosensing scheme in which the sarcosine enzymatic reaction is critical to a tri-enzymatic cascade event. The creatinine sensor yielded sensitivity of ~0.6 μA/mM, similar sensing performance parameters to the sarcosine sensor, and was effectively operated in blood serum at physiologically relevant creatinine concentrations. The demonstrated functionality of these sensors in their respective biological fluids at physiological concentrations of the analyte species suggests potential clinical application as diagnostic tools.

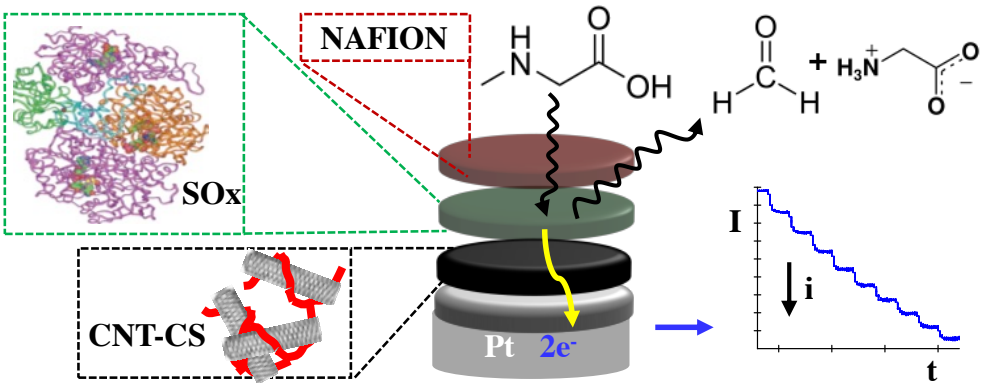

Graphical Abstract

*To whom correspondence should be addressed. Dual corresponding authors. Email: mleopold@richmond.edu: Phone: (804) 287–6329 (MCL) or jpollock@richmond.edu: (804) 484–1578 (JAP). Fax: (804) 287–1897

1. Introduction

Sarcosine is an intermediate in the metabolism of methionine and a by–product in the synthesis and degradation of glycine [1]. As an amino acid derivative, sarcosine serves as a metabolic precursor to many different types of cellular molecules, such as creatine and serine. Preliminary studies have indicated that sarcosine has promise as a possible adjuvant for the treatment of mental illnesses, such as depression and schizophrenia [2, 3]. Sarcosine is also an intermediate in the enzymatic degradation of creatinine and creatine, the former an indicator molecule for the presence of muscular degradation, kidney disease, and possible renal failure [4]. In addition, increased sarcosine levels have been attributed to the development of prostate cancer [5-8].Specifically related to prostate cancer, current medical diagnosis involves the determination of prostate–specific antigen (PSA), a protein directly linked to the presence of prostate cancer. However, the determination of PSA as an indicator for prostate cancer has historically led to over–diagnoses and unreliable results, requiring the use of more invasive procedures, most notably biopsy [9]. With the increased recognition of the importance of sarcosine and its metabolic precursors for potential diagnosis purposes, the scope of sensor development research has also expanded, including both electrochemical [8,10] and spectroscopic [7] strategies. Innovative systems are increasing targeting sarcosine, including recent developments with polymer imprinting [7] and colorimetric assay methods [9, 11]. As such, the need for a sarcosine sensor that is accurate, sensitive, and adaptable to on-site application with widespread use while not requiring costly fabrication or complex instrumentation remains an important goal.

Biosensors featuring electrochemical detection of targeted analyte species offer many of the attributes desired in diagnostic sensors and have extensively explored this possibility for a number of different analytes [12]. In order to ensure selectivity with electrochemical systems, oxidase enzyme–based biosensors offer a viable strategy due to their high specificity toward target analyte as well as their ability to be immobilized onto a surface or within a matrix. Hydrogen peroxide, a by–product of enzyme-catalyzed reactions between target analyte and oxygen, is subsequently oxidized at an electrode surface, creating a reliable amperometric signal directly proportional to analyte concentration. These 1st generation amperometric biosensors have shown success, both with a glucose model system as well as other clinically relevant tested analytes, such as uric acid [13]. While these systems excel in terms of simplicity and affordability, the ability to

adapt these systems to respond to numerous analytes through minimal modification is of particular interest for clinical applications, including the potential to miniaturize the sensors to wire electrodes .

Amperometric biosensing schemes are typically designed to target molecules that are abundant in biological fluids (e.g., amperometric glucose biosensors aim for mM detection levels). As a sensing target, sarcosine is clinically relevant at relatively low concentrations and highlights the need for a more sensitive detection platform. As typical with all biosensor schemes, the signal from a working electrode can be depressed in attempts to provide selectivity to a system by modifying the electrode with functional layers [14]. The use of chitosan as a scaffolding material has been widely researched and integrated into biosensing schemes; the material has many positive attributes: biocompatibility, effective adhesion and absorption onto electrode surfaces, high affinity for aqueous solutions, the ability to incorporate nanomaterials, as well as a chemical structure amenable to synthetic modification at the projected hydroxyl and amino functional groups [15-20].

The incorporation of carbon nanotubes (CNTs) specifically into the chitosan matrix has been of general interest due to their conductive and catalytic properties aimed at enhancing the generally non–conductive chitosan matrix [20]. Multiple methods of incorporation have been studied, including covalently attaching the nanotubes directly to the chitosan matrix as demonstrated by Carson et al. (2009) [21]. However, modification of CNTs was determined to create more defect sites, resulting in lower conductivity and diminished returns in terms of nanotube incorporation [21]. The incorporation of nanomaterials, including CNTs as well as gold colloidal nanoparticles, all of which have unique properties regarding their conductivity, interactions with biological materials, and surface area–to–volume ratio, have been shown to enhance amperometric–based signals at electrode interfaces [14, 22-24]. The collective body of work suggests that nanomaterials provide a convenient solution to the trade–off between sensitivity and selectivity due their stability within a scaffolding material, which would simultaneously immobilize an oxidase enzyme and any stabilizing agents needed. The lower concentrations of sarcosine relative to other typical analytes give special interest into these signal enhancement strategies and materials.

Previous works have found success with the use of sarcosine oxidase (SOx), an enzyme that catalyzes the reaction:

$$Sarcosine + H_2O + O_2 \rightarrow Formaldehyde + Glycine + H_2O_2 \quad (1)$$

often times coupled with the enzymatic reactions of creatininase (CA) and creatinase (CI) [25, 26]. It is notable that one the most important applications of a sarcosine sensor to consider is its ability to function within schemes designed to detect creatininase. While some reports have found success with direct adsorption of SOx on the electrode surface [4], immobilization within a layer–by–layer (LbL) system provides a more intuitive solution for the inclusion of SOx, nanomaterials, and other stabilizing agents previously explored within other systems.

In this work, a LbL approach towards sarcosine detection involving carboxylic acid functionalized carbon nanotube–chitosan nanocomposite films as a scaffold for an enzymatic layer terminated with a Nafion binding layer is demonstrated. While individual sensor reports utilizing CNTs are found throughout the literature, our study separates itself in identifying the properties of the nanomaterials that exert more influence in an effective sarcosine electrochemical sensor. Additionally, after exploring different CNT materials and optimizing the functional ad–layers, the performance of the developed biosensor system is evaluated for sensitivity, selectivity, stability and functionality in relevant bodily fluid samples. Because sarcosine sensing is critical within the indirect detection of creatinine, the sensor developed herein is also assessed as a functional component of a creatinine-sensing scheme. Ultimately, the attributes of our sensing scheme are compared to a very limited number of electrochemical sarcosine sensor reports in the literature [4, 27-31] in order to emphasize the potential promise of this approach for further development toward clinical application.

2. Experimental Section

2.1. Materials and instrumentation

All chemicals were purchased from Sigma–Aldrich unless specifically stated. Nafion (Liquion solution LQ–1105 1100EW 5% wt. and D2021 20% wt.) was purchased from Ion Power, Inc. (New Castle, DE, USA). Pristine and carboxylic acid functionalized single–walled carbon

nanotubes (p–SWCNTs and COOH–SWCNTs) were purchased from NanoLab, Inc. (Waltham, MA, USA). Creatininase enzyme was purchased from BBI Solutions (> 500 U/mg), synthetic urine (Surine) from Cerilliant (Sigma-Aldrich), and blood serum (sheep) from Hemostat. Ultra–purified water (UP H_2O, 18.3 MΩ cm) was used to prepare all solutions. An eight–channel potentiostat (CH Instruments, 1000B) was used to record amperometric current–time (I–t) curves to evaluate the analytical performance of the sensors, as described below. Electrochemical cells were comprised of a common Ag/AgCl (saturated KCl) reference electrode, a common platinum wire counter electrode (Sigma–Aldrich), and modified platinum working electrodes (2mm diameter, CH Instruments). An FT-IR ATR spectrophotometer (Thermo Scientific-Nicolet iS10) was used to characterize either drop-cast (e.g., chitosan solution) or powder (e.g., CNT) samples.

2.2. Sarcosine Oxidase

Protein Expression. The plasmid vector pET–21a encoding for SOx (Genscript) was transformed into chemically competent *E. coli* BL21 (DE3) Star cells (Invitrogen) to express SOx. The transformed Star cells were grown in an overnight culture with 10 mL of terrific broth, supplemented with ampicillin (100 μg/mL). Terrific broth (250 mL) + AMP (100 μg/mL) cultures were inoculated with 2.5 mL of overnight culture. The cultures were then incubated with shaking at 37 ℃ until they reached an OD_{600} of 0.5–0.6. At this point, protein expression was induced with IPTG to a final concentration of 0.1 mM and incubated with shaking for 3 hours at 37℃. Afterwards, the cells were harvested by centrifugation at 4,000 rpm for 30 minutes at 4℃. The pellets were stored at –20℃.

Protein Purification. Cell pellets were re–suspended in 4 mL of lysis equilibration buffer (50 mM NaPi, 200 mM NaCl, 5 mM imidazole, pH 7.6), supplemented with PMSF (0.5 mM). Cells were lysed by sonication, then centrifuged at 12,000 rpm for 30 minutes at 4℃ to remove cellular debris. The crude lysate was purified using a Ni–NTA affinity column. The column was charged with $NiCl_2$ (50 mM) and equilibrated with lysis buffer (50 mM NaPi, 200 mM NaCl, 5 mM imidazole, pH 7.6). The cell lysate was added to the column and washed with wash buffer 1 (50 mM NaPi, 200 mM NaCl, 25 mM imidazole, pH 7.6), followed by wash buffer 2 (50 mM NaPi, 200 mM NaCl, 50 mM imidazole, pH 7.6) Finally, the protein was eluted with elution buffer (50 mM NaPi, 200 mM NaCl, 250 mM imidazole, pH 7.6). The purified SOx was desalted using a 10DG column

(Bio–Rad) into 5 mM phosphate buffer (pH 7.6). This final protein product was analyzed with SDS–PAGE (Supporting Information, Fig. SI–1) before being lyophilized for 24–72 hours.

Enzyme Activity Assay. A hydrogen peroxide fluorescence assay (Sigma Aldrich) was used to assess the functionality and activity of the sarcosine oxidase product, following manufacturer procedures. The assays indicated that the SOx produced in house was fully functional with adequate activity levels (see Supporting Information, Fig. SI–2).

2.3 Preparation of electrode materials

As previously mentioned, chitosan has been used previously for immobilizing enzymes and nanomaterials within biosensing schemes [16-19, 21]. This body of work has extensively characterized the chitosan layers via some combination of UV-Vis, FT-IR and Raman spectroscopies, electrochemical techniques, and electron microscopies [15-16,18,20-21], though the latter techniques seem to offer limited information regarding the CS films. Because of the extent of the CS film characterization available in the literature, exhaustive repetition of all these techniques was not performed in this study. Rather, readily available electrochemical methods and FT-IR spectroscopy was used to simply confirm CNT incorporation into the CS films. CS solution was prepared as previously reported with a slight modification [32]. Briefly, 0.5% wt. CS solution was prepared using stirring for 1 h in 1.0 % acetic acid. The pH was adjusted to 5.0 using drops of 1M NaOH solution. CNTs (1 mg) were added into 1 mL of 0.5 % wt. CS solution (pH 5.0), followed by ultrasonication for 2h to form a suspension of CNTs. The mixture was then separated using centrifugation and the supernatant, comprised of homogeneously dispersed CNTs, was used as the electrode material. Sarcosine oxidase solutions were prepared by dissolving the desired amount of SOx in 4.4 mM phosphate buffer solution (PBS), prepared by mixing mono- and di- potassium phosphate solutions to desired pH of 7.0.

2.4 Electrode preparation

Platinum electrodes (Pt) were successively polished with 1.0, 0.3, and 0.05 μm alumina powder (Electron Microscopy Sciences) and rinsed thoroughly with ultrapure water. Then the electrodes were electrochemically cleaned in 0.1M H_2SO_4 solution via cyclic voltammetry between

–0.4 and +1.2 V vs Ag/AgCl prior to use. As illustrated in **Scheme I**, a typical electrode modification involved a 7.0 μL aliquot of CNT–CS solution being drop–cast on the electrode surface and allowed to dry in 50% RH controlled chamber for 45 min. to obtain Pt/CNT–CS modified electrodes that are visibly darker compared to the clean Pt electrodes. Then a 7.0 μL aliquot of SOx (6 mg/mL) solution was subsequently drop–cast onto the electrode, allowed to dry (50% RH, 60 min.) to obtain Pt/CNT–CS/SOx modified electrode. Finally, a 7.0 μL aliquot of Nafion solution was then drop–cast onto that composite film, allowed to dry (50% RH, 10 min.) to obtain the final Pt/CNT–CS/SOx/Nafion biosensor. The entire process for these and other L-b-L combinations of these materials was conducted at room temperature.

For evaluating the sensors, modified electrodes were submerged in 25.0 mL of phosphate buffer solution (PBS, 4.4 mM, pH 7) stirring at 1100 rpm. The working electrode potential was held at +0.65 V for 1200 seconds prior to consecutive 25 μL injections of 0.25 M sarcosine stock solution at 100 seconds intervals. Stair–step amperometric current time responses were produced as a result of successive 100 μM sarcosine increases. Sensor performance was evaluated using linear regression analysis of calibration curves. As in prior work, slopes of calibration curves (i.e., current response vs. sarcosine concentration) corresponded to sensitivity while response times ($t_{R-95\%}$) were defined as the time required to reach 95% of the total change in current due to an increase in sarcosine concentration [14, 33].

3. Results and Discussion

The overall design of the enzymatic layer–by–layer (LbL) sarcosine electrochemical biosensor is depicted in **Scheme I**, featuring three major components on a platinum electrode interface: (1) carbon nanotubes–chitosan nanocomposite (CNT–CS) layer; (2) sarcosine oxidase enzyme (SOx) layer; and (3) an outer Nafion layer. It should be noted that CNT is used as a general acronym representative of any carbon–based nanomaterial. The following study proceeds by characterizing the modified electrode, evaluating different nanomaterials as a functional components of the scheme, optimization of materials within the layered construction, and culminating with an evaluation of sensor performance, including performance in biological media (e.g., synthetic urine and blood serum) and as part of a creatinine biosensing scheme as well. The performance of the sensor is compared and contrasted to literature reports of sensors for both

sarcosine and creatinine. In general, the use of these components as a composite film was shown to function effectively over a sufficient linear range with high sensitivity, fast response times, and specific selectivity toward sarcosine in a variety of matrices.

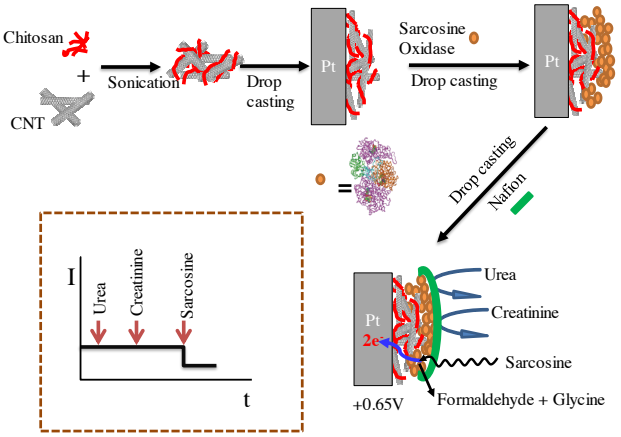

Scheme I: Schematic representation of the LbL sarcosine electrochemical biosensor and idealized current time response toward analyte and interferents

3.1 Nanocomposite film electrode modification

The characterization of potassium ferricyanide $(Fe(CN)_6]^{3-/4-}$ cyclic voltammetry (CV) at modified electrodes remains an effective tool to monitor the progress of adlayers since electron transfer (ET) occurs either by tunneling through an interface (e.g., ET via tunneling through the alkane chain of a self-assembled monolayer) or at defects in the interfacial barrier where solution redox species can access the electrode [34, 35]. In this study, the $Fe(CN)_6^{3-/4-}$ redox probe was chosen to examine changes of electrode surface characteristics upon modification by CS or CNT material. **Figure 1** shows typical CVs and differential pulse voltammetry (DPV) (**inset**) of $Fe(CN)_6^{3-/4-}$ observed at different combinations of the layered materials compared to a bare Pt electrode, the latter exhibiting expected well–defined oxidation and reduction peaks (**Fig. 1a**). The introduction of pristine multi–walled carbon nanotubes (p–MWCNTs) via mixing with the CS material (i.e., p–MWCNT–CS/Nafion/Pt), showed peak current responses comparatively higher than that at the bare Pt electrode. The enhanced amperometric response suggests that the p–MWCNT–CS nanocomposite modified electrodes may benefit from the increased electroactive surface area due to the incorporation of the CNTs, a result consistent with the conclusions of other reports in the literature using these materials [20, 36]. Furthermore, the peak–to–peak potential separation between the cathodic and anodic peaks of the Pt/p–MWCNTs–CS/Nafion is slightly smaller (66

mV) than that of the bare Pt (72 mV), suggesting that the p–MWCNTs–CS are facilitating faster ET kinetics [37].

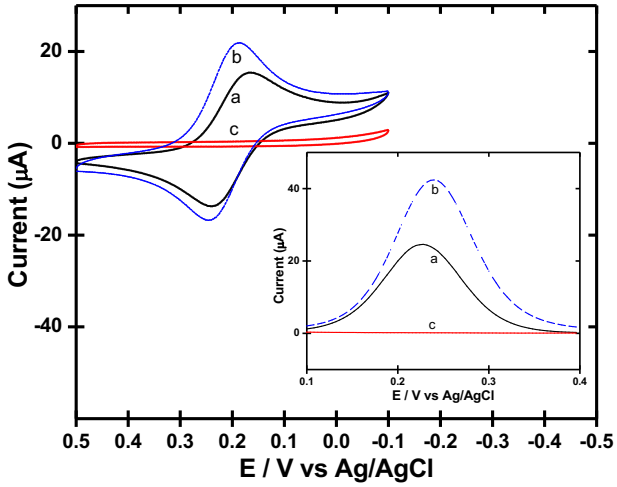

Figure 1: Cyclic voltammetry and Differential pulse voltammetry (**inset**) of 5mM $Fe(CN)_6^{3-/4-}$ (0.5 M KCl) at (a) bare Pt, and (b) p-MWCNT-CS/Nafion, (c) Nafion modified Pt.

Differential pulse voltammetry (DPV), a technique that effectively discriminates against background charging current often observed with CNTs at electrode interfaces, reinforced the CV results, the CS layer and the CS doped with CNTs both show in an enhancement of the redox probe's signal (**Fig. 1, inset)**, consistent with literature [20, 37]. While CNTs, in general, are known to behave electrocatalytically at electrode interfaces [38], the results suggest that the incorporation method and type of CNT may play a role in achieving that effect. Also noteworthy, electrodes modified only with Nafion exhibited severely attenuated voltammetric signals, suggesting that this layer is somewhat selective against diffusional species in solution (**Fig. 1c**). In addition to the electrochemical evidence of successful CNT incorporation at the electrode interface, the CNT-doped chitosan modified electrodes were all visibly darker than the bare platinum electrodes.

Infrared spectroscopy (FTIR) was employed as an additional qualitative confirmation of the successful dispersion of different CNTs within the CS matrices (see Experimental Section 2.1 for method details). **Figure 2a** displays the characteristic IR spectra of CS films where vibrational bands for CS film spectra were assigned based on the previously published data [15, 39] including the broad absorption observed between 3600 cm^{-1} and 3000 cm^{-1} being attributed to OH and NH_2 stretching vibrations. Additionally, distinctive NH_2 bending absorptions at 1651 cm^{-1}, 1557 cm^{-1}, 1374 cm^{-1} as well as the symmetric CH stretching vibrations at 2920 and 2871 cm^{-1} are visible. Absorption bands at 1149 cm^{-1} (anti–symmetric stretching of C–O–C bridge), 1061 cm^{-1}, and 1024

cm^{-1} (skeletal vibration involving the C–O stretching) are characteristics of chitosan's saccharide structure [39]. If a film of CNT-doped CS material is deposited, these FT-IR signature absorptions should persist.

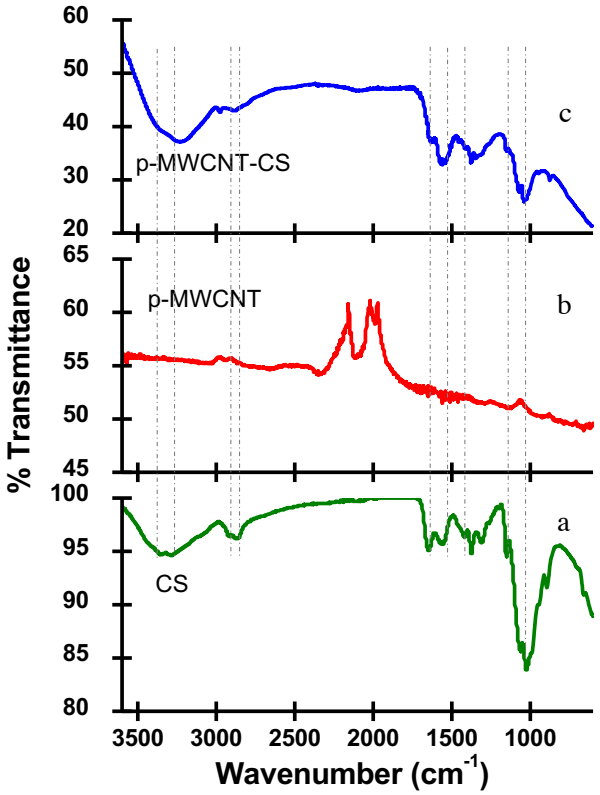

Figure 2: FT-IR spectroscopy characterization of a) CS, b) p-MWCNT, c) p-MWCNT-CS

Typical IR analysis of most CNTs, regardless of their structural nature (e.g., single vs. multi–walled or functionalized vs. pristine), reveal broad-band absorption with few features. For example, **Figure 2b** is a typical spectrum for unfunctionalized or pristine-multi-walled carbon nanotubes (p-MWCNT) – relatively featureless with significantly lower % transmittance compared to the CS film (Fig. 2a). Similar spectra can be collected for p-SWCNT and their functionalized counterparts as well (shown in Supporting Information, Fig. SI-3). Importantly, the FT-IR spectra of the p-MWCNT–CS composite film (**Figure 2c)** shows the persistence of spectral features of CS, including signature peaks of CS at 3360 cm^{-1}, 1149 cm^{-1} and 1024 cm^{-1}. The spectroscopy results suggests that the p-MWCNT is successfully incorporated into the CS matrix. The decrease in transmittance coupled with the spectral signature of CS can be shown in similar comparisons for COOH functionalized MWCNT, SWCNT, and COOH-SWCNT films with CS as well (Supporting Information, SI-3). In the case of COOH functionalized CNTs (both MWCNTs and SWCNTs), the presence of a slight signal at ~1720 cm^{-1} is attributed to the presence of the

carbonyl functional group. The weakness of this peak for these materials suggests that there are low concentrations of carboxylic acid functional groups, most likely localized to the edges of the tubes [40]. This characteristic peak is notably absent in the pristine SWCNT and MWCNT, which is similar to previously observed spectra as well [20, 41].

While IR analysis of the materials allows for a qualitative assessment of the CNTs incorporation within the film, probing voltammetry using $Fe(CN)_6^{3-/4-}$ at these interfaces (**Figure 3**) is consistent with the spectroscopic characterization presented. Regardless of the type of CNT, all of the CNT–CS/Nafion modified platinum electrodes exhibited comparatively higher peak currents for the redox probe than at bare platinum electrodes. As observed in other studies [36, 38, 42, 43], there is an indication that CNT incorporation at an electrode interface results in significant electrocatalytic activity attributed to an increased electroactive surface area [37]. In this study, as well as others [37], COOH–SWCNT–CS modified Pt electrodes (**Fig. 3A, e**) exhibited particularly higher current response and the smaller peak–to–peak potential separation (57 mV) compared to bare Pt and CS/Nafion modified electrodes. It should be noted that enhanced current response obtained with CNTs incorporation was evident regardless of how the voltammetry peaks were analyzed (i.e., isolating Faradaic current manually or background subtracted voltammetry) (see Supporting Information, Fig. SI–4 and Table SI–1).

Chronocoulometry (CC) of the $Fe(CN)_6^{3-/4-}$ probe was also used in order to experimentally support the increased effective electroactive surface area believed to be achieved with CNT incorporation into these films. The electroactive surface areas of the bare Pt, CS and CNT–CS composite modified Pt were assessed using this methodology where charge (coulombs) as a function of time (chrono) [44], was employed as previously described [22] to generate an Anson plot whose slope could be used in equation 2 to calculate A, the electroactive surface area (cm^2):

$$Q = 2nFACD^{1/2}\pi^{-1/2}t^{1/2} \quad (2)$$

where Q is the charge passed (C), n is the number of electrons transferred, F is Faraday's constant (96,500 C/mole), C is $Fe(CN)_6^{3-/4-}$ concentration (5.00 mM in 0.50 M KCl), D is the diffusion coefficient for $Fe(CN)_6^{3-/4-}$ ($7.6 \times 10^{-6} cm^2/s$), and t is the time (s). The CC determined electrode areas from all seven interfaces are included in Supporting Information (Fig. SI-4 and Table SI-1) and indicate that the nearly 4-fold increase in current response observed at COOH-SWCNT-CS

modified electrodes during voltammetry (Fig. 3A) can be directly attributed to an apparent ~3.6-fold increase in effective electroactive surface provided by that CNT-doped interface. A summary of all CC, CV and DPV results are included in the Supporting Information (Table SI–1).

3.2 Evaluation of Nanomaterials for Sarcosine Sensing

The hypothesis of using SWCNTs with COOH functionalization to maximize effective electroactive surface area was explored by incorporating the various types of CNTs (SWCNT vs. MWCNTs; pristine vs. COOH–functionalized) into the sarcosine electrochemical biosensor (Scheme I). That is, each material was incorporated into chitosan solution, deposited at a platinum electrode with the other layers (SOx enzyme and Nafion), and subsequently evaluated as a sarcosine biosensing system. Nafion interfaces at electrode surfaces have been previously shown to be selective for certain analytes [45]. Additionally, prior work in our lab has established that both pristine and carboxylic acid functionalized MWCNTs when dispersed in Nafion polymer resulted in enhanced sensitivity in uric acid sensing systems [36, 43].

Sensor constructs featuring MWCNTs were examined during injections of sarcosine. Common to LbL construction of modified electrodes, initial attempts to utilize these materials consisted of drop–casting the material directly onto the electrochemically cleaned Pt electrodes. **Figure 3B** shows the amperometric I–t curves and the corresponding calibration curves (**inset**) for CS films containing p–MWCNT, COOH–MWCNT as well as control systems without CS (i.e., SOx enzyme and p–MWCNTs/SOx directly deposited at the electrode and capped with a Nafion layer). The control experiments, the films lacking the CS scaffold (i.e., Pt/SOx/Nafion and Pt/p–MWCNT/SOx/Nafion), resulted in extremely poor current responses for sarcosine (i.e., absence of typical stair–step behavior) and an appraised sarcosine sensitivity of only 0.006 (±0.002) μA/mM (**Fig. 3B, a,b**). However, the incorporation of either p–MWCNT or COOH–MWCNTs within the CS layer, subsequently treated and covered with SOx and Nafion (i.e., Pt/p–MWCNT–CS/SOx/Nafion and Pt/COOH–MWCNT–CS/SOx/Nafion), showed expected stair–step current responses and resulted in enhanced sensitivities of 0.08 (±0.00$_4$) and 0.12 (±0.05) μA/mM, respectively (**Fig. 3B, c,d**). The use of COOH–functionalized MWCNTs consistently yielded more defined steps and higher sensitivity, suggesting that the carboxylic acid moieties within the film may allow for effective engagement and coupling of the nanomaterials with the CS scaffold. This

enhanced response may be due to the amine functional groups on the CS, deposited at pH 5 in this study, being cationic and possibly interacting with the negatively charged CNTs during the dispersion process [46].

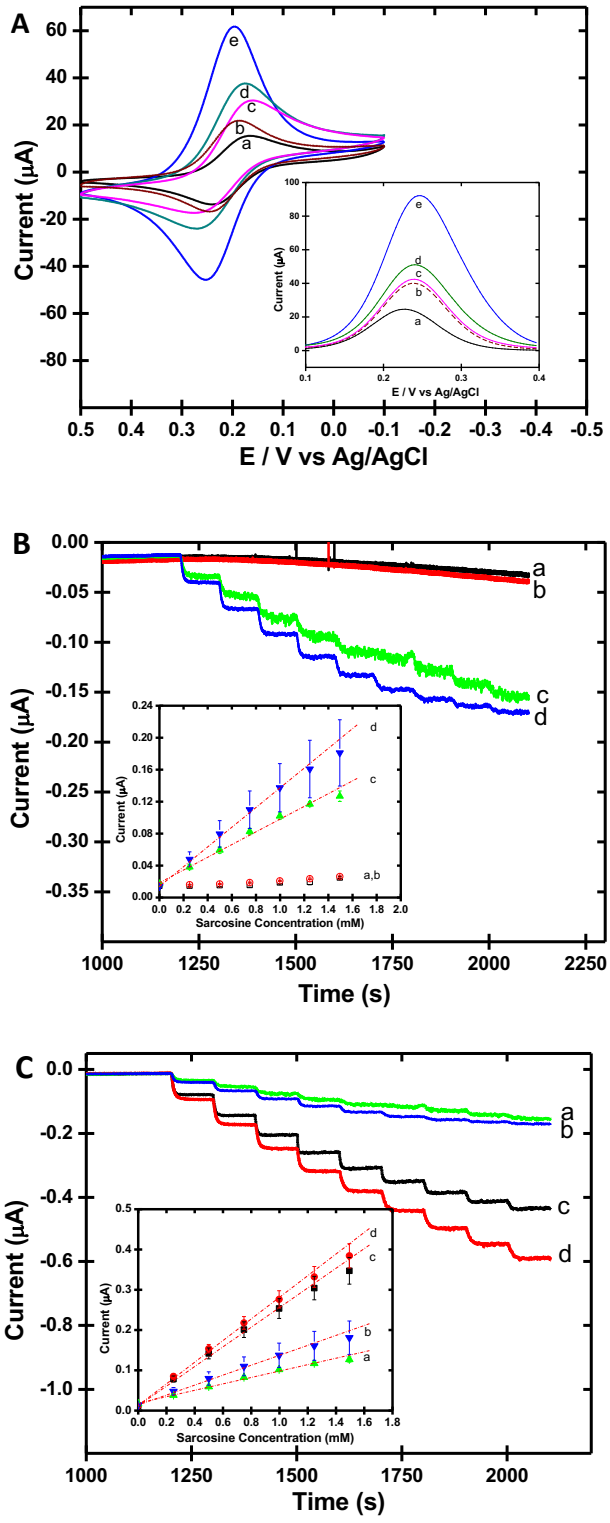

Figure 3: **(A)** Cyclic voltammetry and differential pulse voltammetry (**inset**) of 5 mM $[Fe(CN)_6]^{3-/4-}$ (0.5 M KCl) at (a) bare Pt, and (b) p-MWCNT-CS/Nafion, (c) COOH-MWCNT-CS/Nafion, (d) p-SWCNT-CS/Nafion, (e) COOH-SWCNT-CS/Nafion modified Pt; **(B)** Representative amperometric I-t curves and corresponding calibration curves (**insets**) during successive 0.25 mM injections of sarcosine at Pt electrodes modified with (a) SOx/Nafion, (b) p-MWCNT/SOx/Nafion, (c) p-MWCNT-CS/SOx/Nafion and (d) COOH-MWCNT-CS/SOx/Nafion; or **(C)** platinum electrodes modified with (a) p-MWCNT-CS/SOx/Nafion, (b) COOH-MWCNT-CS/SOx/Nafion, (c) p-SWCNT-CS/SOx/Nafion and (d) COOH-SWCNT-CS/SOx/Nafion. Nafion concentration was 5% in all cases. Note: Solid symbol markers indicate a step-like response and, in some cases, standard error bars are smaller than markers for average value (n = 3–5).

With a preliminary result suggesting that the critical component of the sensing scheme may be the CNTs, additional variations of the material were incorporated with the CS matrix within the sarcosine biosensing scheme, including both p–SWCNTs and COOH–SWCNTs. SWCNTs are known for superior electrical conductivity [47]. **Figure 3C** shows the comparative effects the various types of CNTs on the electrocatalytic activity of the LbL sarcosine biosensor in terms of amperometric I–t responses and corresponding calibration curves. Indeed, the correlation between sensitivity and type of CNT utilized is affirmed. The use of SWCNT in CNT–CS nanocomposites, regardless of COOH functionalization, resulted in significantly higher sensitivities (0.22 ±0.05 μA/mM and 0.25 ±0.04 μA/mM, respectively) compared to biosensors schemes with the MWCNTs. The substantial increase in sensitivity may be due to the higher conductivity property of SWCNT [47]. Additionally, the smaller diameter of the SWCNTs compared to MWCNTs potentially allows for a greater surface concentration of SWCNTs to be drop–cast onto the electrode surface in the same deposition volume (i.e., 7 μL); this effect may contribute to the sensitivity enhancement as well. From the collective findings, COOH–SWCNTs were selected as the optimal material for this study. Substantial control experiments were conducted where individual layers or materials (e.g., Nafion, the CNTs, CS) were omitted in the constructs and tested for sarcosine response. The only systems to yield a stair–step current response with significant sensitivity toward sarcosine were those systems with all four components: CS with CNTs, SOx and Nafion (Supporting Information, Fig. SI–6).

3.3. SOx and Nafion Optimization

In order to optimize the performance of the electrochemical biosensor, other parameters that may affect the electrochemical biosensor activity were examined. To understand the effect of enzyme concentration, various amounts of SOx, between 2 and 10 mg/mL, in 4.4 mM PBS (pH 7.0) were applied in the sensor design via drop–casting directly onto the optimal COOH–SWCNT–CS nanocomposite interface. Calibration curves (**Figure 4A**) generated from corresponding I–t responses (Supporting Information, Fig. SI–7) show that with lower concentrations of SOx (e.g., 2 mg/mL), sensitivity is low (0.05 ±0.03 μA/mM). However, as the concentration of SOx was increased to 4 mg/mL and 6 mg/mL, sensitivity was observed to increase three and nearly six–fold, respectively. For concentrations beyond 6 mg/mL sensitivity drops off again (~0.16–0.17

μA/mM). The observed decrease in sensitivity at higher SOx concentration may be due to an increased thickness of the enzyme layer itself hindering the substrate from reaching the active site.

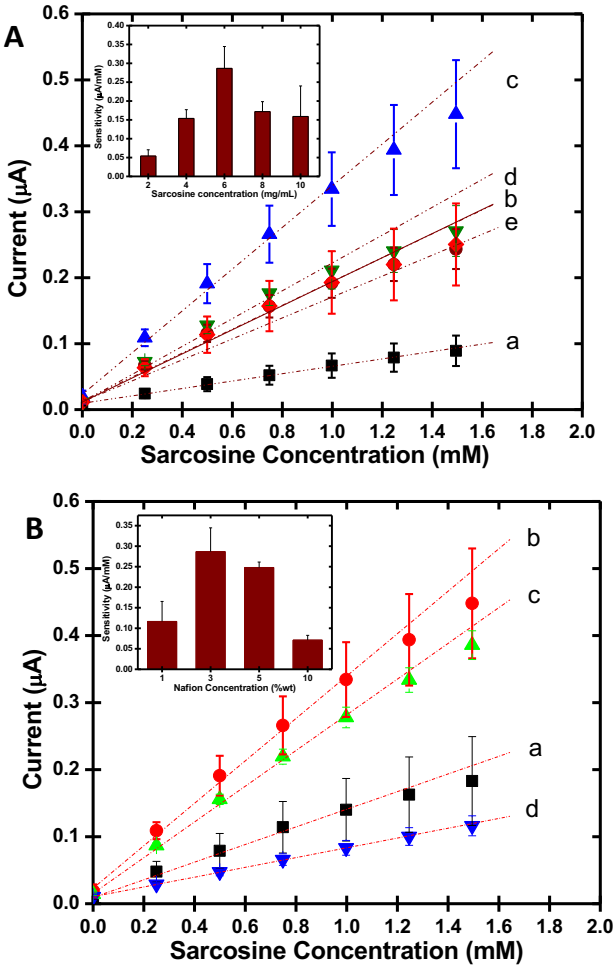

Figure 4: Calibration curves obtained from the amperometric I-t curve during successive 0.25 mM injections of sarcosine at **(A)** Pt/COOH-SWCNT-CS/SOx/Nafion using various concentrations of SOx: (a) 2 mg/mL, (b) 4 mg/mL, (c) 6 mg/mL, (d) 8 mg/mL and (e) 10 mg/mL with a summary bar graph of measured sensitivities (**inset**). Nafion concentration was 5% in all cases; **(B)** Pt/COOH-SWCNT-CS/SOx/Nafion with various concentrations of Nafion: (a) 1 % wt., (b) 3 % wt., (c) 5 % wt. and (d) 10 % wt. with a summary bar graph of measured sensitivities (**inset**). Note: Solid symbol markers indicate a step-like response and, in some cases, standard error bars are smaller than markers for average value (n = 3–4).

Similarly, the concentration of the outer Nafion layer was examined by using deposition solutions of varying concentration, 1 to 10 wt % Nafion in ethanol at the Pt/COOH–SWCNT–CS/SOx/Nafion system. **Figure 4B** displays typical calibration curves (I–t responses provided in Supporting Information, Fig. SI–8) obtained from the application of various Nafion concentrations. A sensitivity of 0.12 (±0.08) μA/mM was observed when 1% wt. of Nafion was applied. However, the sensitivity of the electrochemical biosensor was increased ~2.5X when the concentration of Nafion was increased to 3% wt. Films tested with between 3–5% generally exhibited baseline noise reduction as well, with 5% Nafion coatings often yielding the lowest noise. This type of noise reduction has been observed previously when polyurethane [13-14, 36]

and Nafion [42] have been employed as part of LbL modification of biosensing electrodes. At Nafion coatings greater than 5%, however, the signal was markedly attenuated and sensitivity decreased, likely due to the increased thickness of the film hindering the accessibility of the sarcosine to the detection mechanism.

3.4. Biosensing Performance

The LbL composite films featuring the layers of COOH–SWCNT–CS, 6 mg/mL SOx and 3% wt. Nafion exhibited the highest average sensitivity (0.29 ±0.12 μA/mM), a dynamic/linear range up to 1.5 mM sufficient for physiological levels of sarcosine, and a limit of detection ($3\sigma_{blank}/b_{1}$) of 13.0 $\pm 0.0_{156}$ μM. Additionally, the optimized sarcosine biosensing system showed an excellent response time ($t_{R-95\%}$) of ~8 seconds, a conservative estimate of the response where the time is measured once 95% of the total current change is achieved [14, 33]. As part of evaluating system performance, the selectivity or influence of interfering species on the detection of sarcosine was investigated. Selectivity assessment of Pt/COOH–SWCNT–CS/SOx/Nafion electrochemical biosensor is shown in **Fig. 5A** where the complete film is subjected to injections of common interferents, along with sarcosine, to reaffirm sensitivity toward analyte in the presence of interfering species. As seen in the I–t curves (**Fig. 5A**), injections of the most common interfering species, urea and creatinine, did not result in significant current responses (0.25 ±0.01 nA and 0.35 ±0.01 nA, respectively) relative to the observed average sarcosine current response (298.0 ±0.2 nA) which is order of magnitude higher. Similar insignificant current responses an order of magnitude smaller than at the compiled films were observed for the interferents at bare platinum electrodes (Supporting Material, Fig. SI-9), suggesting that the compounds may be gaining minor access to the electrode through the films.

As has been done in previous studies [14, 33, 48, 49], selectivity coefficients (K^{amp}) can be used to conservatively and quantitatively assess selectivity using the following equation:

$$K_j^{amp} = \log\left(\frac{\Delta I_j / C_j}{\Delta I_{Sarcosine} / C_{Sarcosine}}\right) \tag{3}$$

where ΔI_j and $\Delta I_{sarcosine}$ are the measured step currents for a specific interferent species (j) and sarcosine (see Supporting Material for specific current measurements) and C_j and $C_{sarcosine}$ are

concentrations of the interferent species and sarcosine, respectively. Selectivity coefficients are useful when evaluating sensors because they allow for a normalized concentration comparison of analyte signal versus interferent response. Negative selectivity coefficients indicate that the interferent is inconsequential whereas species with positive values are indicative of the selective species. **Fig. 5A (inset)** displays a graphical comparison of initial (Day 0) selectivity coefficients of +0.21, –2.91, and –3.31 calculated for sarcosine, urea, and creatinine, respectively, for the Pt/COOH–SWCNT–CS/SOx/Nafion biosensing system. The selectivity coefficient for sarcosine is measured comparing the response of the 0.25 mM injection to that of a three-fold higher injection (0.75 mM) into Equation 3.

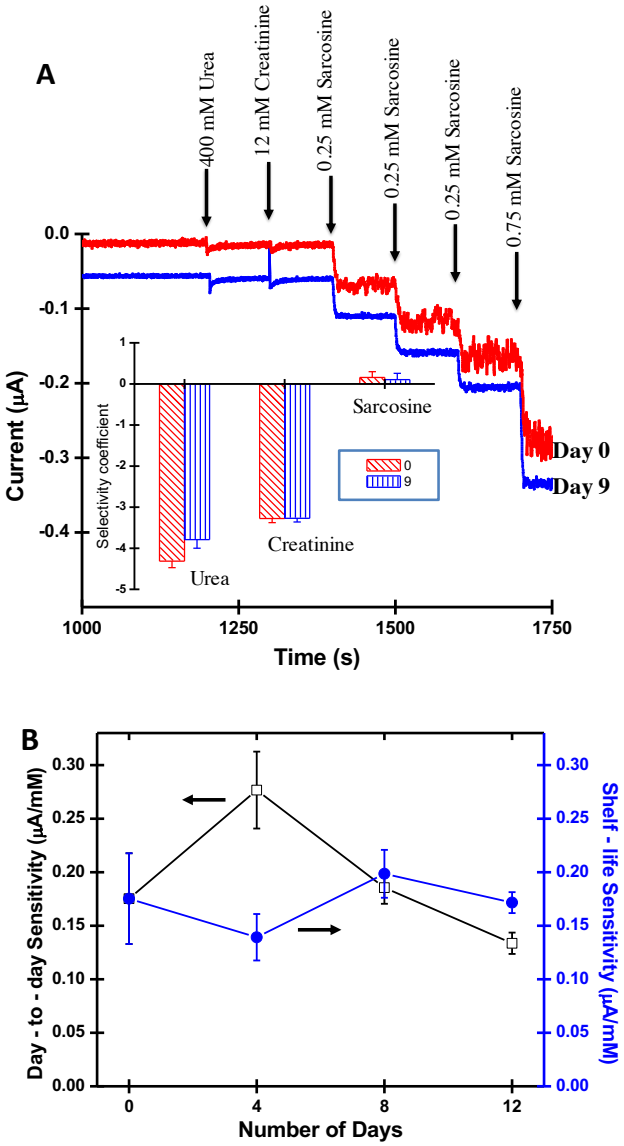

Figure 5: (A) Typical amperometric I-t curves of Pt/COOH-SWCNT-CS/SOx/Nafion electrochemical biosensor during injections of common interferent species and sarcosine and a graphical summary (inset) of selectivity coefficients for urea and creatinine on day 0 and day 9. (n = 6). Note: Day 9 I-t is offset by 50 nA for viewing; **(B)** Day-to-day (continuous use) and shelf life (single use) sensitivity tracking for a set (n=4) of sarcosine biosensors (Pt/COOH-SWCNT-CS/SOx/Nafion).

As part of their sensing performance, the stability of the sarcosine biosensors functionality over time was evaluated in two important ways. First, the sensors were evaluated for continuous use stability, where sensitivity toward sarcosine for a set of the same electrodes was monitored day-to-day. The recorded sensitivity of the same set of sensors undergoing daily testing revealed general stability for at approximately one week before degradation was observed (i.e., lower sensitivity) – **Fig. 5B**. While sensitivity did eventually degrade over the course of twelve days, the sensors remained remarkably selective for sarcosine in the presence of urea and creatinine during the same timeframe, yielding selectivity coefficients of +0.11, –3.28, and –3.27 at day 9, respectively (**Fig.5A, inset**).

However, given the nature of the targeted sarcosine–related illnesses (e.g., prostate cancer) and the type of physiological samples readily available from patients seeking diagnosis (e.g., urine and blood), continuous measurement of sarcosine *in vivo* is not as desirable as with other analytes such as glucose (diabetes) or uric acid (pregnancy–induced hypertension/preeclampsia risk) [14, 36, 43]. Similarly, the stability of reusing the same electrodes for repeated, day-to-day sarcosine measurements is of less significance. It is much more relevant to test the shelf–life sensitivity of individual sensors that would be employed for single measurements of bodily fluids samples. More specifically, and in contrast to the aforementioned daily or continuous testing, a number of electrodes were fabricated on the same day and stored. Each day a new, previously *unused* (i.e., aged) composite film was evaluated for sarcosine sensitivity. The results of the shelf–life assessment (**Fig. 5B**) indicate that sensors, stored at 7-8°C and aged up to nearly two weeks maintained their effective sensitivity toward sarcosine.

While limited in number, literature reports of other sarcosine sensors exist and it is important to place the sensor developed herein in context. A table summary of the performance of the complete optimized system (Pt/COOH–SWCNT–CS/SOx/Nafion) and comparison of these properties to other related literature reports of sarcosine or sarcosine–related sensors is provided in Supporting Information (Table SI–3). The collective sensing performance of the optimized sensor in this study is comparable with other sarcosine sensors in the literature, equaling or exceeding standard sensing parameters such as sensitivity, linear sensing range, response time, and limit of detection, though details of how the latter parameters were measured are not easily ascertained in some reports. Few reports offer as rigorous evaluation of selectivity or as

conservative of a response time measurement or shelf–life evaluation - all critically important to eventual application. Additionally, this study takes the additional step to transition the sensing capability to biological matrices (see below).

During the course of the study, exploration of different combinations of the materials and deposition strategies uncovered minor alterations in biosensor construction that modestly, but significantly, improved the sarcosine sensitivity. First, it was found that the initial layering of CS, followed by the deposition of COOH–SWCNTs, designated as Pt/CS/COOH–SWCNT/SOx/Nafion, as opposed to depositing a pre-made mixture of the two materials, designated Pt/CS-COOH-SWCNT/SOx/Nafion, increased sarcosine sensitivity by ~30% (see Table SI-3, Supporting Information). No other specific layering of the materials resulted in a similar enhancement of the signal (Supporting Information, Fig. SI–6, Table SI–3). This result suggests that the proximity or bridging of the SWCNTs between SOx and the CS layer is critical. In addition to this specific layering effect, doping the outer Nafion layer with additional enzyme also enhanced sensor signal as has been observed in other reports [27]. This effect is illustrated in comparing the same systems with and without SOx doped Nafion (Supporting Information, Fig. SI-10). The highest sustained observed sarcosine sensitivity (0.40 to 0.50 μA/mM) was recorded with films incorporating both of these alterations (i.e., Pt/CS/COOH–SWCNT/SOx/Nafion*, where the asterisk indicates additional doping with SOx – see Table SI-3) – a system subsequently employed for critical sarcosine measurements of the study, including those made in biological fluids such as urine (see below).

3.5. Biosensor Operation in Bodily Fluids

The specific medical application of the presented sensors will depend on the ultimate goal of the diagnosis. For example, in detecting sarcosine as an early indication for prostate cancer, sensor functionality in urine samples and the ability to respond to abnormal concentrations of sarcosine (>20 μM) is required [46]. In order to evaluate the applicability of the developed electrochemical biosensor for such an application, sensors were tested in synthetic urine media and sarcosine-spiked urine samples were quantitatively assessed. **Figure 6** shows the calibration curve derived from I-t responses during sarcosine injections of a number of electrodes with Pt/CS/COOH–SWCNT/SOx/Nafion films in buffer. The sensitivity of the response is as expected,

but when this calibration curve is used to assess a synthetic urine test sample, which has been spiked with 1.5 mM sarcosine, the average detection of sarcosine by the sensor is only 0.19 (±0.13) mM both with and without background (charging current) correction. The severely depressed measurement of the spiked sample suggests detrimental matrix effects that can be corrected for by matrix matching the calibration. The same film constructs, calibrated in synthetic urine (**Fig. 6**) resulted in relative lower sensitivity but more quantitative accuracy when inserted into the sarcosine-spiked sample of synthetic urine (1.5 mM). The sensor exhibited a well-defined amperometric step (Supporting Information, Fig. SI-11 and 12), a response that translated against the calibration curve with much more accurate sarcosine concentration determination of 1.42 (±0.13) mM and 1.35 (±0.9) mM before and after charging current correction, respectively. This result establishes effective percent recovery (≥ 90% in both cases) as well as low relative percent error (~ 5%).

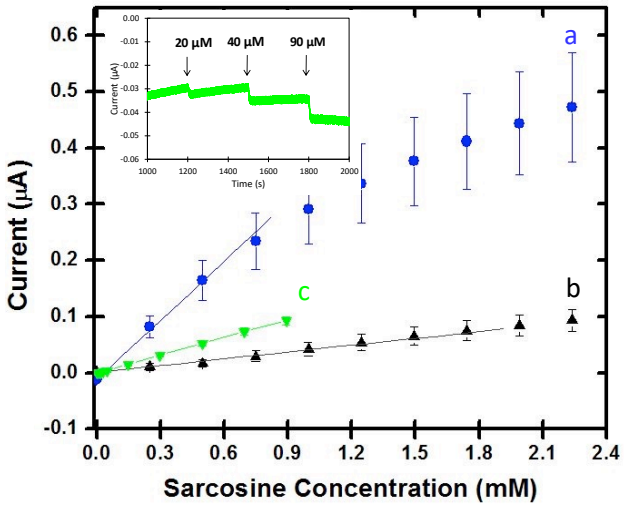

Figure 6: Calibration curves obtained from amperometric I-t curves during successive 0.25 mM injections of sarcosine at Pt/CS/COOHSWCNT/SOx/Nafion (3%) in (a) 4.4 mM potassium phosphate buffer (pH 7; n = 4) compared to (b) synthetic urine (n = 4), and (c) variable injections of 50 mM sarcosine at Pt/CS/COOH-SWCNT/SOx/Nafion*(3%) in synthetic urine (n = 5); **Inset:** Example of amperometric response to 20, 40, and 90 μM sarcosine spiked synthetic urine samples at Pt/CS/COOHSWCNT/SOx/Nafion*(3%).

Notes:* indicates that the layer is doped with additional SOx; In some cases, standard error bars are smaller than markers for average value; Calibration curve (c) shown in Supporting Information.

Based on prior successful enhancement of signal, the same system with an additional doping of SOx into the outer Nafion layer (Pt/CS/COOH–SWCNT/SOx/Nafion*) was also tested in synthetic urine. As shown in Figure 6, the enhancement is readily apparent in this media as well with the improved slope of the calibration curve (Supporting Information, Fig. SI-13). In order to be a clinically relevant sensor for prostate cancer diagnosis via urine analysis, the sarcosine sensors need to be accurate at micromolar concentrations of sarcosine (≥ 20 μM). As a proof-of-concept experiment, sensors were used to measure the sarcosine concentration of a limited number of spiked synthetic urine samples at 20, 40, and 90 μM. All three concentrations were easily detected

by the Pt/CS/COOH–SWCNT/SOx/Nafion* sensors during the I-t scan with representative results shown in **Fig. 6** (**inset**). In general, the sensors performed admirably, effectively quantifying the sarcosine in the more complex matrix at micromolar levels (**Table 1**). The results of using sensors in spiked synthetic urine samples show that, for most samples, high percent recovery and low relative error were achieved on a significant number of sensors.

Table 1. Sensor Performance in Sarcosine Spiked Samples of Synthetic Urine (Pt/CS/COOH-SWCNT/SOx/Nafion*)

Sarcosine-Spiked Urine Sample Concentration (μM)	**Measured Sarcosine Concentration** (μM)	**n**	**Average % Recovery**	**Average % Relative Error**
20	19.7 (±0.9)	9	98.5	-1.5%
40	41 (±2)	7	102.5	+2.5%
90	94 (± 9)	3	104.4	+4.4%

Notes: * Indicates a layer doped with additional SOx; Uncertainty represents standard deviation.

While being uniquely suited for incorporation into sarcosine detection platforms, such as the one we have presented, SOx is also widely utilized in creatinine detection systems. Creatinine represents an analyte that has been targeted for the diagnosis of, among other diseases, impending renal failure and muscle degradation [4]. Creatinine biosensor designs have found success with a tri–enzymatic cascade reaction involving creatininase (CI), creatinase (CA), and SOx [25, 26, 30]:

$$\begin{aligned} \text{Creatinine} + H_2O \text{ –CI} &\rightarrow \text{Creatine} \\ \text{Creatine} + H_2O \text{ –CA} &\rightarrow \text{Sarcosine} + \text{Urea} \\ \text{Sarcosine} + H_2O + O_2 \text{ –SOx} &\rightarrow H_2O_2 + \text{Formaldehyde} + \text{Glycine} \end{aligned} \quad (4)$$

It follows then that the versatility of any developed sarcosine biosensing scheme will be inherently linked to its ability to function within a creatinine biosensor, ultimately affecting the significance of the sensor development. Ideally, an electrode featuring this tri–enzyme cascade would be operational in blood or blood serum, allowing for a potential *in vitro* diagnostic tool. Although blood testing requires more considerations, such as accounting for additional natural and artificial interferents (e.g., uric acid, acetaminophen, respectively), the higher relevant concentrations of

creatinine indicative of nephron malfunction (>1 mM) is amenable to the sensor developed in this study [50]. Here, we report the adaptation of our sarcosine biosensing scheme to be a functional component of the tri–enzymatic scheme for creatinine. Essentially, the enzymatic layer of our scheme replaces the SOx layer with a layer of combined SOx, creatinase, and creatininase enzymes (**Scheme II**). Prior to being incorporated into the scheme, all enzymes were tested for activity

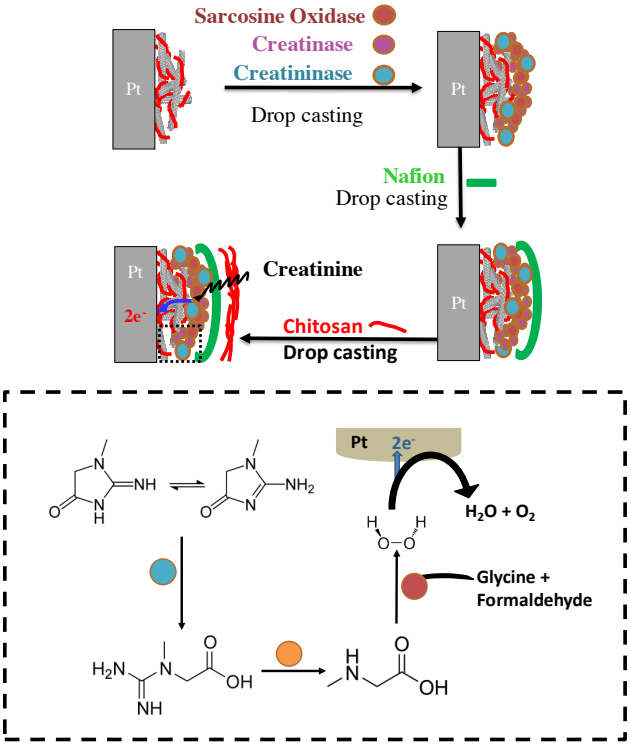

Scheme 2: Schematic representation of the LbL creatinine biosensing scheme featuring the sarcosine sensor as a functional component.

with a fluorometric assay (Supporting Information, Fig. SI-14). The tri-enzyme combination was deposited on Pt/CS/COOH-SWCNT interfaces and capped with Nafion before testing for creatinine sensitivity in phosphate buffer. **Figure 7** shows the system was clearly responsive to creatinine injections in buffer (0.04 μA/mM) while the same experiment, conducted in blood serum, yielded significantly attenuated creatinine sensitivity (0.008 μA/mM), the same type of sensitivity depression observed for the sarcosine sensor when the testing media was changed from buffer to urine (Fig. 6). With the sarcosine/urine testing, manipulation of the outermost semi-permeable membrane resulted in an improved signal-to-noise ratio and ultimately improved sensitivity in that matrix. Biosensor schemes utilizing other types of materials such as sol-gels have established that the introduction of a diffusional layer often achieves better sensor

performance, including lower noise, greater sensitivity, and lower limits of detection [13, 14, 49]. A similar effect is observed here with the creatinine system when an additional, outer diffusional layer of CS (**Scheme 2**). Adding the additional CS layer resulted in significant enhancement of the creatinine sensor performance in buffer, including a creatinine sensitivity of 0.57 μA/mM (not shown in Fig. 7, see Supporting Information, Table SI-3). The enhancement of the performance with the outer CS layer then allowed for the sensor to maintain effective sensitivity when immersed in blood serum (Fig. 7c). serves to lower noise, significantly improving sensitivity back to 0.04 μA/mM, and allowing for a low limit of detection (0.20 ±0.08 mM) and spanning the physiologically relevant creatinine concentrations for disease diagnosis (~ 1 mM).

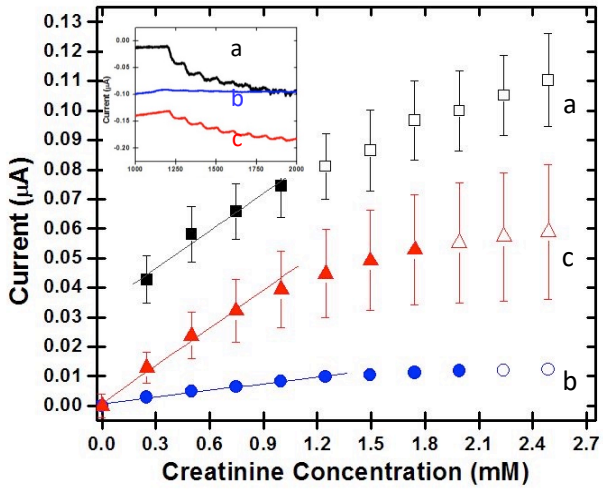

Figure 7: Calibration curves obtained from amperometric I-t curves during successive 0.25 mM injections of creatinine at Pt/CS-COOH-SWCNT/CI-CA-SOx/Nafion in (a) 4.4 mM potassium phosphate buffer (pH 7) and (b) blood serum; (c) the same system with an additional CS capping layer (Pt/CS-COOH-SWCNT/CI-CA-SOx/Nafion/CS) tested in blood serum (buffer response of CS capped system not shown). Note: Solid symbol markers indicate a step-like response (n = 3-6); **Inset:** Corresponding examples of amperometric steps to 0.25 injections of creatinine from the three systems.

The reason for the improved performance achieved with the CS capping layer is not fully understood but, as with other diffusional layers in biosensing schemes [13, 14, 49], the CS layer may be effectively gating the approach and partition of creatinine and/or oxygen into the film and allowing the enzymes to avoid saturation effects. It is also possible that the chitosan may provide additional discrimination against interferents simply improving signal-to-noise. A creatinine calibration curve was collected in blood serum and used to quantify 0.75 mM and 1.0 mM creatinine spiked samples. A typical I-t curve, the step current responses of the spiked samples, and a representative calibration curve are included in Supporting Information (Fig. SI-15). The 0.75 mM and 1.0 mM creatinine spiked solutions were determined to contain 0.765 mM and 1.07 mM creatinine, respectively, both under 10% relative error with high (100-110%) percent recovery on a limited number of tests. The demonstrated functionality of the scheme in blood serum at

clinically relevant concentrations of creatinine is in line with further development of the system toward *in vitro* testing as a medical diagnosis tool.

4. Conclusion

In this work, we have presented a functional LbL electrochemical biosensing scheme for the effective detection of sarcosine as well as a functional component of a creatinine sensor, both systems applicable for numerous clinical diagnoses. The demonstrated LbL approach of this study allows for individual shortcomings of the materials to be overcome, such as the non–conductivity of chitosan and the non–solubility of CNTs. The sensing performance of our system is comparable to other electrochemical schemes with optimization showing that the system has a linear range of detection throughout relevant concentrations, selectivity against interfering molecules, a shelf life amenable to actual clinical application, and successful performance in bodily fluids. The presented biosensing scheme is versatile and robust, allowing additional measures to be applied for greater sensitivity, including signal enhancement via the addition of platinum black modified electrodes [14] and nanoparticle networks [33]. While effective, non-electrochemical sarcosine sensors, some requiring significant materials preparation and intricate fabrication (e.g., nanoparticles [10], quantum dots [51]) as well as complex instrumentation [7], amperometric biosensors continue to maintain advantages of simplicity, cost-effectiveness, and versatility. In the latter regard, electrochemical biosensors of this nature can be adapted to microelectrodes for real-time operation at the patient's bedside [52] or detection of sarcosine in delicate brain tissue, as would be required if used for schizophrenia and depression diagnoses [2,3]. As such, the presented biosensing scheme and the greater understanding of the materials used in the strategy, demonstrate a sensor design poised for further research and a promising candidate for clinical application development.

Keywords: biosensor; sarcosine; creatinine; layer-by-layer; carbon nanotube; 1st generation

Acknowledgments

This research was generously supported by funding from the National Science Foundation (CHE–1401593), Virginia's Commonwealth Health Research Board, the Beckman Foundation (MJP) as well as Camille & Henry Dreyfus Foundation, Henry Dreyfus Teacher Scholar Award, the Floyd D. and Elisabeth S. Gottwald Endowed Chair of Chemistry, and the University of Richmond (JAP). This work was conducted in honor of Phil Joseph, Robert Plymale, and Tammy Hicks - all of whom are vital to the success of the undergraduate research program at the University of Richmond.

References

[1] O. Josypčuk, J. Barek, B. Josypčuk, Construction and Application of Flow Enzymatic Biosensor Based of Silver Solid Amalgam Electrode for Determination of Sarcosine, Electroanal. 27 (2015) 2559-2566.
[2] C.-C. Huang, I.H. Wei, C.-L. Huang, K.-T. Chen, M.-H. Tsai, P. Tsai, R. Tun, K.-H. Huang, Y.-C. Chang, H.-Y. Lane, G.E. Tsai, Inhibition of Glycine Transporter-I as a Novel Mechanism for the Treatment of Depression, Biol. Psychiatry. 74 (2013) 734-741.
[3] D. Strzelecki, M. Podgórski, O. Kałużyńska, L. Stefańczyk, M. Kotlicka-Antczak, A. Gmitrowicz, P. Grzelak, Adding Sarcosine to Antipsychotic Treatment in Patients with Stable Schizophrenia Changes the Concentrations of Neuronal and Glial Metabolites in the Left Dorsolateral Prefrontal Cortex, Int.ernational J. Mol. Sci. 16 (2015) 24475.
[4] Y. Yang, S. Mu, The bioelectrochemical response of the polyaniline sarcosine oxidase électrode, J. Electroanal. Chem. 415 (1996) 71-77.
[5] A. Sreekumar, L.M. Poisson, T.M. Rajendiran, A.P. Khan, Q. Cao, J. Yu, B. Laxman, R. Mehra, R.J. Lonigro, Y. Li, Metabolomic profiles delineate potential role for sarcosine in prostate cancer progression, Nature. 457 (2009) 910-914.
[6] A.P. Khan, T.M. Rajendiran, A. Bushra, I.A. Asangani, J.N. Athanikar, A.K. Yocum, R. Mehra, J. Siddiqui, G. Palapattu, J.T. Wei, G. Michailidis, A. Sreekumar, A.M. Chinnaiyan, The Role of Sarcosine Metabolism in Prostate Cancer Progression, Neoplasia. 15 (2013) 491-IN413.
[7] Z. Heger, N. Cernei, S. Krizkova, M. Masarik, P. Kopel, P. Hodek, O. Zitka, V. Adam, R. Kizek, Paramagnetic nanoparticles as a platform for FRET-based sarcosine picomolar detection, Sci. Reports. 5 (2015).
[8] E.B. Özkütük, S.E. Diltemiz, Ş. Avcı, D. Uğurağ, R.B. Aykanat, A. Ersöz, R. Say, Potentiometric sensor fabrication having 2D sarcosine memories and analytical features, Mater. Sci. Eng. C. 69 (2016) 231-235.
[9] J. Lan, W. Xu, Q. Wan, X. Zhang, J. Lin, J. Chen, J. Chen, Colorimetric determination of sarcosine in urine samples of prostatic carcinoma by mimic enzyme palladium nanoparticles, Anal. Chim. Acta. 825 (2014) 63-68.

[10] T.P. Nguy, T. Van Phi, D.T. Tram, K. Eersels, P. Wagner, T.T. Lien, Development of an impedimetric sensor for the label-free detection of the amino acid sarcosine with molecularly imprinted polymer receptors, Sens. Actuators B. Chem. 246 (2017) 461-470.
[11] Z. Xue, H. Wang, H. Rao, N. He, X. Wang, X. Liu, X. Lu, Amperometric indicator displacement assay for biomarker monitoring: Indirectly sensing strategy for electrochemically inactive sarcosine, Talanta. 167 (2017) 666-671.
[12] J. Wang, Amperometric biosensors for clinical and therapeutic drug monitoring: a review, J. Pharm. Biomed. Anal. 19 (1999) 47-53.
[13] G.E. Conway, R.H. Lambertson, M.A. Schwarzmann, M.J. Pannell, H.W. Kerins, K.J. Rubenstein, J.D. Dattelbaum, M.C. Leopold, Layer-by-layer design and optimization of xerogel-based amperometric first generation biosensors for uric acid, J. Electroanal. Chem. 775 (2016) 135-145.
[14] M.B. Wayu, M.J. Pannell, M.C. Leopold, Layered Xerogel Films Incorporating Monolayer-Protected Cluster Networks on Platinum-Black-Modified Electrodes for Enhanced Sensitivity in First-Generation Uric Acid Biosensing, ChemElectroChem. 3 (2016) 1245-1252.
[15] R. Nanda, A. Sasmal, P. Nayak, Preparation and characterization of chitosan–polylactide composites blended with Cloisite 30B for control release of the anticancer drug paclitaxel, Carbohydr. Polym. 83 (2011) 988-994.
[16] J. Lin, C. He, Y. Zhao, S. Zhang, One-step synthesis of silver nanoparticles/carbon nanotubes/chitosan film and its application in glucose biosensor, Sens Actuators B. Chem. 137 (2009) 768-773.
[17] J. Tkac, J.W. Whittaker, T. Ruzgas, The use of single walled carbon nanotubes dispersed in a chitosan matrix for preparation of a galactose biosensor, Biosens. Bioelectron. 22 (2007) 1820-1824.
[18] X. Kang, J. Wang, H. Wu, I.A. Aksay, J. Liu, Y. Lin, Glucose Oxidase–graphene–chitosan modified electrode for direct electrochemistry and glucose sensing, Biosens. Bioelectron. 25 (2009) 901-905.
[19] X.-L. Luo, J.-J. Xu, Y. Du, H.-Y. Chen, A glucose biosensor based on chitosan–glucose oxidase–gold nanoparticles biocomposite formed by one-step electrodeposition, Anal. Biochem. 334 (2004) 284-289.
[20] B.K. Shrestha, R. Ahmad, H.M. Mousa, I.-G. Kim, J.I. Kim, M.P. Neupane, C.H. Park, C.S. Kim, High-performance glucose biosensor based on chitosan-glucose oxidase immobilized polypyrrole/Nafion/functionalized multi-walled carbon nanotubes bio-nanohybrid film, J. Colloid Interface Sci. 482 (2016) 39-47.
[21] L. Carson, C. Kelly-Brown, M. Stewart, A. Oki, G. Regisford, Z. Luo, V.I. Bakhmutov, Synthesis and characterization of chitosan–carbon nanotube composites, Mater. Lett. 63 (2009) 617-620.
[22] L.T. DiPasquale, N.G. Poulos, J.R. Hall, A. Minocha, T.A. Bui, M.C. Leopold, Structure–function relationships affecting the sensing mechanism of monolayer-protected cluster doped xerogel amperometric glucose biosensors, J. Colloid Interface Sci. 450 (2015) 202-212.
[23] A.R. Schmidt, N.D.T. Nguyen, M.C. Leopold, Nanoparticle Film Assemblies as Platforms for Electrochemical Biosensing—Factors Affecting the Amperometric Signal Enhancement of Hydrogen Peroxide, Langmuir. 29 (2013) 4574-4583.
[24] S. Hrapovic, Y. Liu, K.B. Male, J.H.T. Luong, Electrochemical Biosensing Platforms Using Platinum Nanoparticles and Carbon Nanotubes, Anal. Chem. 76 (2004) 1083-1088.

[25] S. Yadav, R. Devi, P. Bhar, S. Singhla, C.S. Pundir, Immobilization of creatininase, creatinase and sarcosine oxidase on iron oxide nanoparticles/chitosan-g-polyaniline modified Pt electrode for detection of creatinine, Enzyme Microb. Technol. 50 (2012) 247-254.
[26] J. Schneider, B. Gründig, R. Renneberg, K. Cammann, M. Madaras, R. Buck, K.-D. Vorlop, Hydrogel matrix for three enzyme entrapment in creatine/creatinine amperometric biosensing, Anal. Chim. Acta. 325 (1996) 161-167.
[27] T.S.C.R. Rebelo, C.M. Pereira, M.G.F. Sales, J.P. Noronha, J. Costa-Rodrigues, F. Silva, M.H. Fernandes, Sarcosine oxidase composite screen-printed electrode for sarcosine determination in biological samples, Anal. Chim. Acta. 850 (2014) 26-32.
[28] U. Lad, G.M. Kale, R. Bryaskova, Sarcosine oxidase encapsulated polyvinyl alcohol-silica-AuNP hybrid films for sarcosine sensing electrochemical bioelectrode, J. Electrochem. Soc. 161 (2014) B98-B101.
[29] A. Ramanavicius, Amperometric biosensor for the determination of creatine, Anal. Bioanal. Chem. 387 (2007) 1899-1906.
[30] V. Serafín, P. Hernández, L. Agüí, P. Yáñez-Sedeño, J.M. Pingarrón, Electrochemical biosensor for creatinine based on the immobilization of creatininase, creatinase and sarcosine oxidase onto a ferrocene/horseradish peroxidase/gold nanoparticles/multi-walled carbon nanotubes/Teflon composite electrode, Electrochim. Acta. 97 (2013) 175-183.
[31] S. Yadav, A. Kumar, C.S. Pundir, Amperometric creatinine biosensor based on covalently coimmobilized enzymes onto carboxylated multiwalled carbon nanotubes/polyaniline composite film, Anal. Biochem. 419 (2011) 277-283.
[32] H.-M. Huang, P.-K. Huang, W.-H. Kuo, Y.-H. Ju, M.-J. Wang, Sol–gel immobilized enzymatic glucose biosensor on gold interdigitated array (IDA) microelectrode, J. Sol-Gel Sci. Technol. 67 (2013) 492-500.
[33] M.H. Freeman, J.R. Hall, M.C. Leopold, Monolayer-Protected Nanoparticle Doped Xerogels as Functional Components of Amperometric Glucose Biosensors, Anal. Chem. 85 (2013) 4057-4065.
[34] A.A. Karyakin, E.E. Karyakina, H.-L. Schmidt, Electropolymerized Azines: A New Group of Electroactive Polymers, Electroanal. 11 (1999) 149-155.
[35] H. Finklea, Electrochemistry of organized monolayers of thiols and related molecules on electrodes, Electroanal. Chem. A Series Adv. 19 (1996) 109-335.
[36] M.B. Wayu, L.T. DiPasquale, M.A. Schwarzmann, S.D. Gillespie, M.C. Leopold, Electropolymerization of β-cyclodextrin onto multi-walled carbon nanotube composite films for enhanced selective detection of uric acid, J. Electroanal. Chem. 783 (2016) 192-200.
[37] B. Fang, C. Zhang, W. Zhang, G. Wang, A novel hydrazine electrochemical sensor based on a carbon nanotube-wired ZnO nanoflower-modified electrode, Electrochim. Acta. 55 (2009) 178-182.
[38] J.M. Schnorr, T.M. Swager, Emerging Applications of Carbon Nanotubes, Chem. Mater. 23 (2011) 646-657.
[39] X.H. Xu, G.L. Ren, J. Cheng, Q. Liu, D.G. Li, Q. Chen, Self-assembly of polyaniline-grafted chitosan/glucose oxidase nanolayered films for electrochemical biosensor applications, J. Mater. Sci. 41 (2006) 4974-4977.
[40] C. Kim, K. Seo, B. Kim, N. Park, Y.S. Choi, K.A. Park, Y.H. Lee, Tip-functionalized carbon nanotubes under electric fields, Phys. Rev. B. 68 (2003) 115403.

[41] N.G. Sahoo, H. Bao, Y. Pan, M. Pal, M. Kakran, H.K.F. Cheng, L. Li, L.P. Tan, Functionalized carbon nanomaterials as nanocarriers for loading and delivery of a poorly water-soluble anticancer drug: a comparative study, Chem. Commun. 47 (2011) 5235-5237.
[42] M.B. Wayu, J.E. King, J.A. Johnson, C.C. Chusuei, A Zinc Oxide Carbon Nanotube Based Sensor for In Situ Monitoring of Hydrogen Peroxide in Swimming Pools, Electroanal. 27 (2015) 2552-2558.
[43] M.B. Wayu, M.A. Schwarzmann, S.D. Gillespie, M.C. Leopold, Enzyme-free uric acid electrochemical sensors using β-cyclodextrin-modified carboxylic acid-functionalized carbon nanotubes, J. Mater. Sci. 52 (2017) 6050-6062.
[44] A. Bott, W. Heineman, Chronocoulometry, Curr. Sep. 20 (2004) 121-126.
[45] X. Cao, L. Luo, Y. Ding, D. Yu, Y. Gao, Simultaneous determination of dopamine and uric acid on nafion/sodium dodecylbenzenesulfonate composite film modified glassy carbon electrode, J. Appl. Electrochem. 39 (2009) 1603-1608.
[46] M.M. Hasani-Sadrabadi, E. Dashtimoghadam, F.S. Majedi, S. Wu, A. Bertsch, H. Moaddel, P. Renaud, Nafion/chitosan-wrapped CNT nanocomposite membrane for high-performance direct methanol fuel cells, RSC Adv. 3 (2013) 7337-7346.
[47] A. Lekawa-Raus, J. Patmore, L. Kurzepa, J. Bulmer, K. Koziol, Electrical Properties of Carbon Nanotube Based Fibers and Their Future Use in Electrical Wiring, Adv. Funct. Mater. 24 (2014) 3661-3682.
[48] N.G. Poulos, J.R. Hall, M.C. Leopold, Functional Layer-By-Layer Design of Xerogel-Based First-Generation Amperometric Glucose Biosensors, Langmuir. 31 (2015) 1547-1555.
[49] A. Koh, Y. Lu, M.H. Schoenfisch, Fabrication of Nitric Oxide-Releasing Porous Polyurethane Membranes-Coated Needle-type Implantable Glucose Biosensors, Anal. Chem. 85 (2013) 10488-10494.
[50] EH. Taylor (1989) Clinical Chemistry, John Wiley and Sons, New York, 58–62
[51] M. Riedel, G. Göbel, A.M. Abdelmonem, W.J. Parak, F. Lisdat, Photoelectrochemical sensor based on quantum dots and sarcosine oxidase, ChemPhysChem. 14 (2013) 2338-2342.
[52] D.L. Robinson, B.J. Venton, M.L. Heien, R.M. Wightman, Detecting subsecond dopamine release with fast-scan cyclic voltammetry in vivo, Clin. Chem. 49 (2003) 1763-1773.